Desalination and Water Treatment
www.deswater.com

doi:10.5004/dwt.2018.23012

131 (2018) 66–74
November

Investigation of pilot scale manufacturing of polysulfone (PSf) membranes by wet phase inversion method

Serkan Guclu[a,b], Jalal-Al-Din Sharabati[a,b], Farzin Saffarimiandoab[a,b], Meltem Agtas[a,b], Derya Y. Imer[a,b], Mehmet E. Pasaoglu[a,b], Yusuf Z. Menceloglu[c,d], Serkan Unal[c,d], Ismail Koyuncu[a,b,*]

[a]*Environmental Engineering Department, Istanbul Technical University, 34469, Istanbul, Turkey, email: gucluse@itu.edu.tr (S. Guclu), sharabati@outlook.com (J.-A.-D. Sharabati), saffari101@gmail.com (F. Saffarimiandoab), agtas@itu.edu.tr (M. Agtas)*
[b]*National Research Center on Membrane Technologies (MEM-TEK), Istanbul Technical University, 34469, Istanbul, Turkey, email: imerd@itu.edu.tr (D.Y. Imer), mpasaoglu@itu.edu.tr (M.E. Pasaoglu), koyuncu@itu.edu.tr (I. Koyuncu)*
[c]*Sabanci University Nanotechnology Research and Application Center, 34956, Istanbul, Turkey, email: yusufm@sabanciuniv.edu (Y.Z. Menceloglu)*
[d]*Sabanci University Integrated Manufacturing Technologies Research and Application Center & Composite Technologies Center of Excellence, 34906, Istanbul, Turkey, email: serkanunal@sabanciuniv.edu (S. Unal)*

Received 24 April 2018; Accepted 18 August 2018

ABSTRACT

Membranes are used as a support layer for the fabrication of thin film composite membranes. Support layer properties can affect many performance parameters of TFC membranes such as flux, rejection, morphology and stability against pressure. Although studies in lab scale fabrication exist, investigation the pilot scale polysulfone membrane fabrication has not been done. In this study, optimization of polysulfone support membranes fabrication was conducted in pilot scale. Coagulation bath temperature; casting speed and solution content were selected as main parameters for the optimization. Membrane surface properties were investigated in details with SEM and pore size distribution. Membrane performance were determined with permeability experiments. Differences in pilot scale and lab scale membrane manufacturing were observed and compared with literature. On the contrary to literature it was found that, coagulation bath temperature has exact opposite effect in pilot scale membrane formation compared to lab scale studies. 10°C drop (from 25°C to 15°C) in coagulation bath temperature decreased mean pore size of membranes from 27 nm to 8 nm and permeability from 464 l/m²h to 100 l/m²h while everything else was kept constant.

Keywords: Pilot scale membrane production; Sponge-like structure; Non-solvent induced phase separation; RO support layer fabrication; Polysulfone membrane

1. Introduction

Understanding the relationship between structure-performance in membrane science is required for the development of membrane materials. Structural and physico-chemical properties of a membrane determine its separation performance. Besides, the resistance to compaction at high pressures is important for high pressure required membrane processes such as reverse osmosis (RO) which is also dependent on the intrinsic membrane structure.

Developments in membrane science lead the commercialization of high performance RO membranes. Obtaining of high performance from RO membranes was fundamentally determined by developing appropriate membrane structure. A review from 1981 by Cadotte & Petersen - two pioneers of thin film composite membranes - explained developments that lead to production of RO membranes [1].

*Corresponding author.

They described how the idea twisted from the use of low flux Loeb-Sourirajan RO membranes based on cellulose acetate to the development of thin-film composite (TFC) membranes which comprised of a compaction resistant support structure and a salt rejecting active layer.

The Loeb-Sourirajan method is an essential membrane fabrication method for anisotropic membranes. On the other hand, for the development of TFC membranes, it was known that support layer should have an anisotropic structure where small pores on the skin and a much thicker and more permeable micro-porous support for mechanical strength. It's reported in the literature that surface porosity of support membrane has great effect on the permeability of thin-film composite reverse osmosis membranes [2]. In addition, separation performance of reverse osmosis membranes is influenced by support membrane porosity [3]. Surface pore characteristics also play an important role to increase interfacial adhesion between active layer and support [4]. Polyamide active layer formation is affected by pore size of support membrane [5]. Cadotte et al. stated that if average pore size of 20 nm is enough for the formation of defect free reverse osmosis layer [6].

There are several membrane preparation methods like sintering, stretching, track-etching, template leaching, dip coating and phase inversion. Phase inversion is much more preferred and industrially used technic among them [7]. In order to achieve the desired support membrane structure, asymmetric membranes having dense skin layer needs to be developed by immersion precipitation phase seperation (also known as nonsolvent induced phase separation (NIPS)). It is one of the most popular membrane fabrication methods because it allows the preparation of different membrane morphologies in a controlled manner [7]. Phase inversion is suitable for a wide range of synthetic material like polymers. In addition, this technic is suitable for inorganic additives too, such as carbon nanotubes, silver, titania [8–10]. Polysulfone (PSf) is usually used in phase inversion due to its prominent features such as commercially available, having good processibility [11]. In addition to this, PSf chemical structure includes bisphenol-a moiety which allows PSf compatible with polyamide active layer and prevents peeling off polyamide layer from surface of membrane [12].

There are several organic solvents used in membrane manufacturing via phase separation. N-methylpyrrolidone (NMP) [13–18], N,N-dimethylacetamide (DMAc) [15,16, 19–21] and N,N-dimethylformamide (DMF) [22,23] are the most preferred solvents for PSf membrane manufacturing.

Sponge-like membranes compact less than finger-like membranes under high pressures and result in little deformation [24]. So, sponge like membranes are preferred in high pressure applications like TFC-RO membranes. Sponge-like structure can be promoted by extending solvent evaporation time [25,26], adding some additives to coagulation bath [27–28], increasing polymer content in polymer solution [25,29–33], adding nonsolvent to the polymer solution [26,33–37], adding organic additives into polymer solution [38–39] and choosing low miscible solvent/nonsolvent duplexes [28,34].

Although polysulfone support membrane properties were investigated in lab scale for the formation of RO membranes in the literature, no studies have been done for the fabrication of polysulfone support layer in pilot scale. This study investigates the pilot scale fabrication of polysulfone support membranes that can be used for the fabrication of TFC membranes in further studies. For this purpose, the effects of casting parameters were investigated and the differences in membrane structures were discussed by comparing pilot scale to lab scale production. It was aimed to obtain sponge-like membrane structure and smaller pore size on the membrane surface.

2. Materials and methods

2.1. Chemicals and materials

Udel P3500 LCD MB Polysulfone (Mw: 80000–86000 Da) was purchased from Solvay Chemical Company. Dimethylformamide (DMF) used as solvent (AKSA Chemical Company). CU424 type PET used as non-woven (1 m wide) (Neenah Papers). Two types of Polyvinylpyrrollidone (PVP) was used as pore former, PVP 10 (Mw: 10000 Da) and PVP 40 (Mw: 40000 Da) (Sigma Aldrich).

2.2. Pilot scale membrane manufacturing

Non-solvent induced phase separation method was used to produce flat sheet membranes. For the preparation of casting solutions, proper amount of PVP (Table 1) was added to DMF solvent and solution was mixed until no aggregates were observed. Then, polysulfone was added to the solution and was stirred at 65°C for 24 h. Polysulfone concentration was 18 wt% in all casting solutions. An ultrasonic bath was used to remove micro bubbles in solution.

A pilot scale membrane production line was used in membrane production (Fig. 1). System allows producing 1 m wide membrane in desired length and thickness can be adjusted precisely using micrometers. Two baths exist, first bath has a capacity of 1 m^3 and used for coagulation, second bath has a capacity of 0.5 m^3 and used for washing. Coagulation bath is continuously fed with fresh water to remove solvent coming from exchange between solvent and non-solvent, water, during membrane formation.

There are some parameters that should be controlled during pilot scale membrane production (Fig. 2). Tap water was used as the non-solvent and no additives were used in coagulation and washing baths to keep the fabrication process economically feasible since volumes of baths are high. In Table 1, membrane casting parameters were presented. Coagulation bath temperature; solvent evaporation time; casting speed; evaporation time and casting solution composition were changed to obtain desired pore size. Gap between nonwoven support and casting blade was fixed to 50 µm. Three different coagulation bath temperatures (15°C, 25°C, and 30°C) were examined. To prevent pore collapse, membranes were washed with 10% glycerol and 90% water as reported in literature before [40].

2.3. Characterization of membranes

Surface and cross-section morphological characterizations of membranes were examined using Quanta FEG 250 scanning electron microscope. All samples were dried prior

Table 1
Membrane manufacturing parameters

Code	PVP10 (%)	PVP40 (%)	Casting speed m/min	Solvent evaporation time	Bath temperature
M1	4.5	1.5	0.5	53 s	30
M2	4.5	1.5	1	26 s	30
M3	4.5	1.5	1.5	18 s	30
M4	4.5	1.5	2	13 s	30
M5	4.5	1.5	2	13 s	25
M6	4.5	–	2	13 s	25
M7	2.5	–	2	13 s	25
M8	2.5	–	3	9 s	25
M9	2.5	–	3	9 s	15
M10	4.5	–	3	9 s	25
M11	4.5	–	3	9 s	15

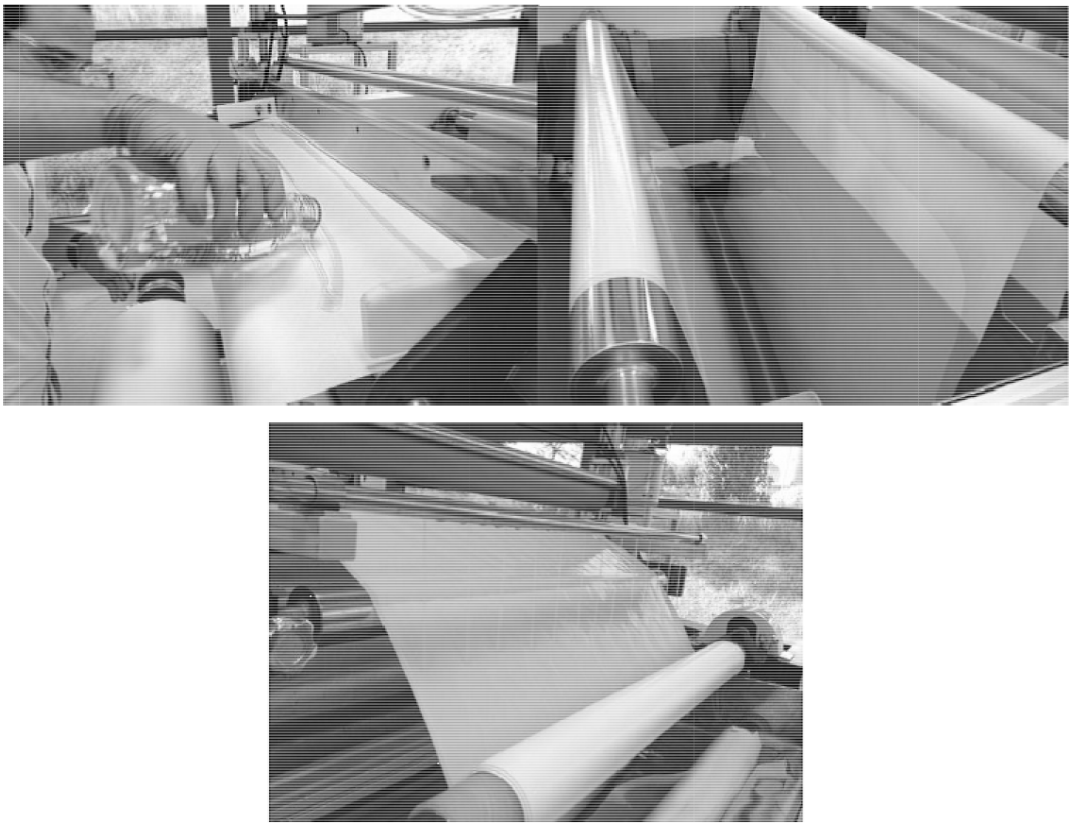

Fig. 1. Production of PSf support layer membranes using a pilot scale casting machine.

to coating. All samples were coated with about 5 nm thick layers of Au-Pd using Quorum SC7620 ion sputtering. Pore size distributions were done using Image J software.

2.4. Membrane performance

The pure water permeability of the membranes was determined by dead-end filtration cells (Sterlitech Corp., Kent, USA). Each membrane area was 14.3 cm^2. All membranes were compacted at least one hour before flux tests under 3 bar to obtain steady state flux. For each membrane, pure water flux was calculated using the following equation:

$$J = \frac{V}{A\Delta t} \tag{1}$$

where V is the volume of permeate (L), A is the effective membrane area (m^2), and Δt is the permeation time (h).

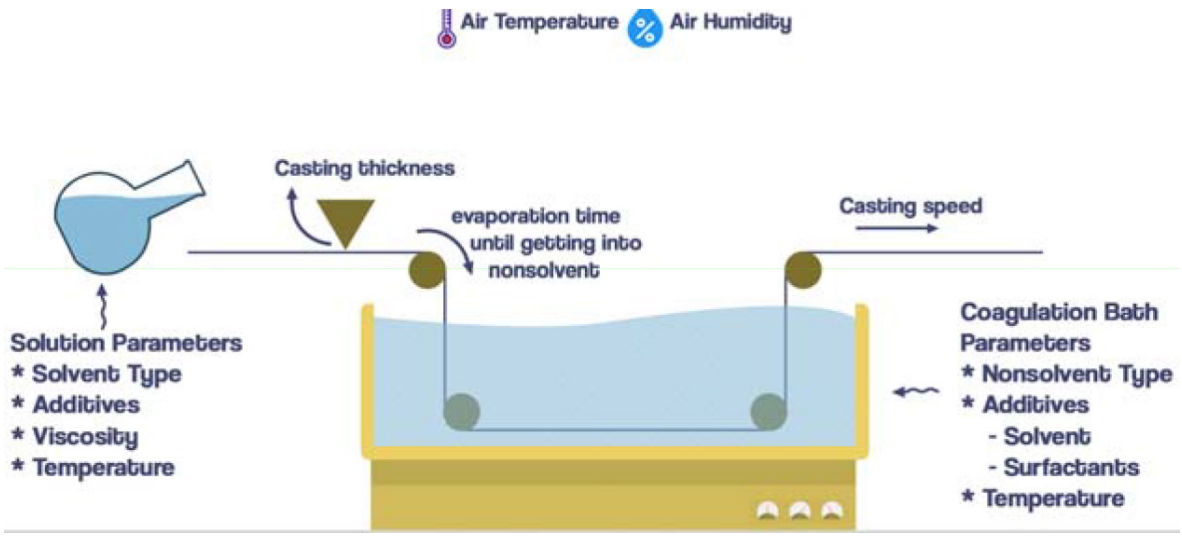

Fig. 2. Parameters affecting pilot scale membrane formation.

Membrane permeability was determined based on flux values measured at three different transmembrane pressures.

3. Results and discussion

3.1. Morphological evaluation of membranes

SEM images of membrane surfaces, and processed images of these surfaces obtained from Image J software are given in Fig. 3. Processed images were used to determine pore sizes and pore size distributions of the produced membranes. Also, in Fig. 4, cross section morphologies of the produced membranes are given. Arrows in Fig. 3 and Fig. 4 show the effects of casting parameters. Red arrows were used to show the effects of solvent evaporation times and membrane casting speeds. At red arrow direction, membrane casting speed increases whereas solvent evaporation time decreases. Blue arrows show the effects of temperature decrease in coagulation bath. Green arrow shows the effects of decreased PVP amount on the membrane morphology. M1 and M2 membranes have more sponge structures as explained in further section. Any pore formation was not visually observed. While evaporation time decreases from M3 to M4, M7 to M8 and M6 to M10, pore sizes decreased as can be seen in SEM images.

Regarding Fig. 3, membranes were formed with longer evaporation time, dense structures were observed (M1 and M2). On the other hand, when the evaporation time decreases and casting speed increases, the formation porous top layer was observed (M3 and M4). It has been known that solvent evaporation time affects membrane formation directly since final membrane structure in phase inversion is mainly determined by the top surface of casted membrane solution film [41]. When evaporation time increases, more solvent evaporation is expected from the top layer of the membranes. Using slow casting speed allowed the solvent to evaporate much more before the casting solution immersed into the coagulation bath, caused a higher concentration of the polymer as a thin film on top of the polymer solution. When solution is immersed into water, the denser structure on the top surface decreased the rate of water intrusion and slows the exchange rate between solvent and non-solvent. In addition, slower casting speed increased the duration of casting solution exposure to air humidity which is an important parameter for membrane formation. Due to humidity, on top surface of the membranes, polymer precipitates and polymer rich layer is observed. This gel layer is more viscous than other parts of casted polymer solution. This viscous gel layer can decrease the de-mixing rate and in turn exchange rate between solvent and non-solvent decrease too [11]. It can be said that if evaporation time decreases, exchange rate between solvent and non-solvent will be increased. This will result in the formation of polymer rich phase on membrane surface having small and tight pores. When the situation is vice versa, formation of dense top layer and sponge-like structures are expected.

Green arrow shows the effect of PVP amount on the membrane morphology. It can be inferred from Fig. 3 that decreasing the PVP amount in casting solution altered the rate of phase inversion and led to increase in the amount of smaller and tighter pores on membrane surface. Guillen et al. stated that, increasing the PVP amount in casting solution enhances sponge-like formation [11].

Blue arrows show the effects of coagulation bath temperature on membrane morphology. It has been known that, decreasing coagulation bath temperature, decreases de-mixing rate. Therefore, bigger pores and sponge-like structure is expected [42]. However, according to the Fig. 3 and Fig. 4, results contradicted with the expected results. Membranes with higher coagulation bath temperature have more sponge like structure. While coagulation bath temperature decreased during manufacturing of membranes M4 to M5, M8 to M9 and M10 to M11, membrane pore sizes decreased and much asymmetric structure was observed. This can be explained by slow de-mixing occurred when membranes were formed. Membrane forming time after immersion of casting solution into coagulation bath gives precipitation rate. If membrane formation completes quickly and casting solution turns opaque, that means precipitation rate is higher.

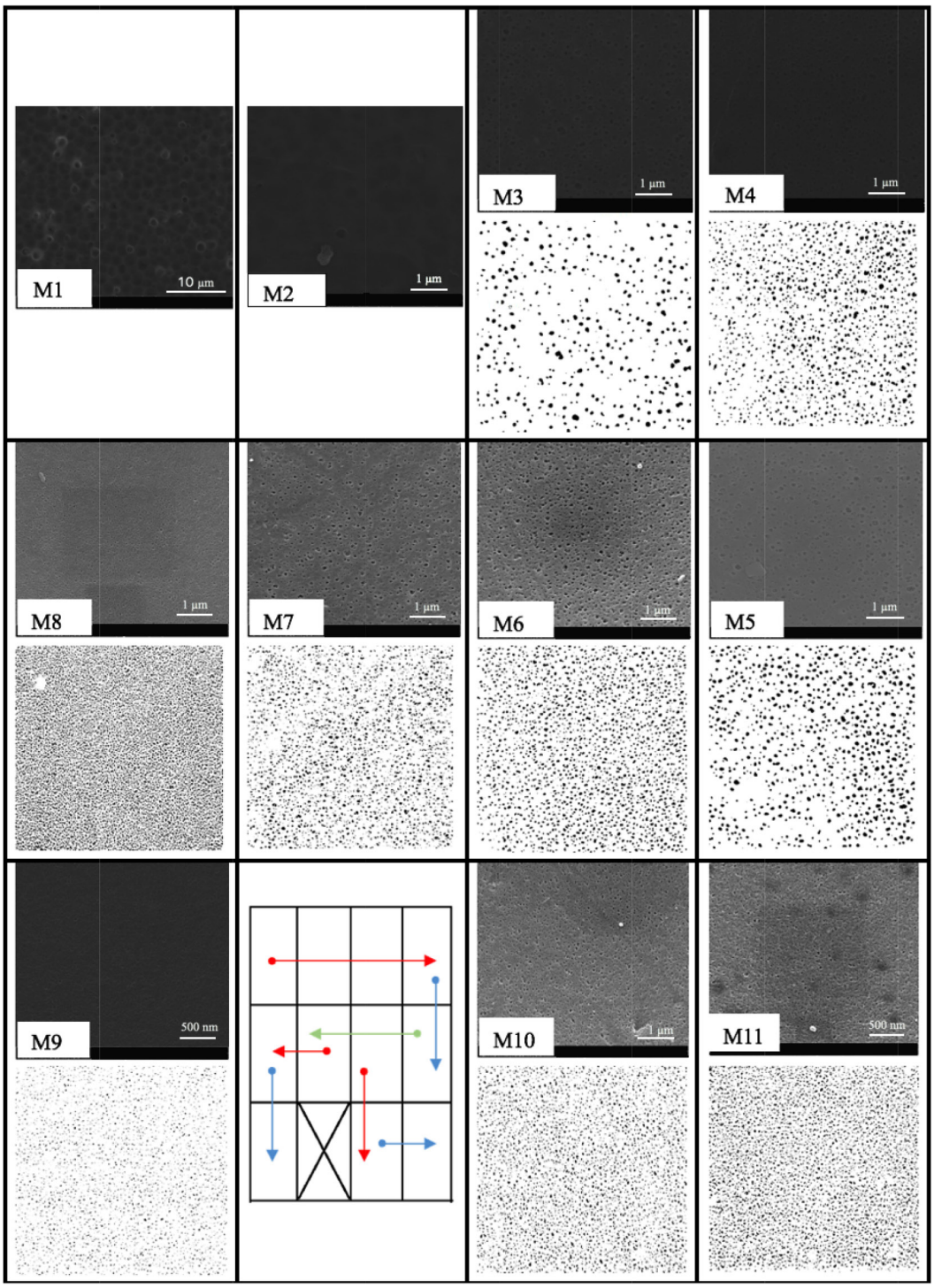

Fig. 3. SEM images of membrane surfaces and extracted pore images.

Formation of sponge-like morphologies enhanced in slower precipitation rates [27]. Therefore, it is expected that more asymmetric structure should be observed in higher coagulation bath temperatures. But it seemed that as coagulation bath temperature decreases, increase in the formation of asymmetric structure was observed opposed to the literature. It is stated that increased coagulation bath temperatures resulted in wide finger-like macro voids [42]. This may be explained by continuous pilot scale membrane fabrication can be different than batch lab scale membrane fabrication.

To understand what can be the reason for the differences obtained in pilot and lab scale membrane production, humidity was measured at different levels of the coagulation

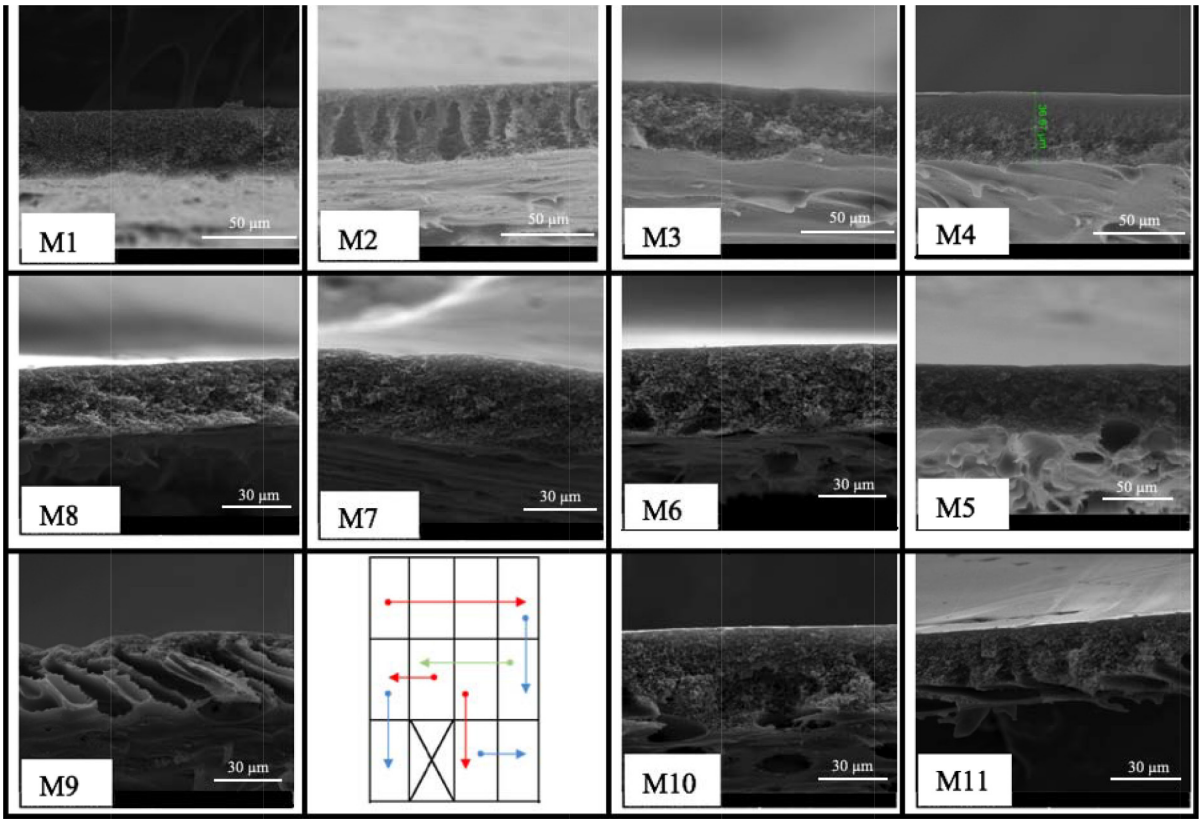

Fig. 4. Cross section SEM images of membranes.

Table 2
Average temperature and relative humidity values

Data point ⇒	Casting knife		5 cm over bath	
Coagulation bath temperature ⇓	Average temperature (C°)	Humidity (%)	Average temperature (C°)	Humidity (%)
15	23.9	34	23.8	35
25	24.1	36	24.7	41
30	24.2	36	26.1	49

bath and results were given in Table 2. Han et al. showed that, 1–2% of water can decrease the time to reach cloud point for PSf-DMF-water systems [41]. Therefore, it can be concluded that PSf-DMF solutions are tend to coagulate rapidly and phase inversion completed quickly. Increasing coagulation bath temperature increased air humidity in the vicinity of coagulation bath. Humidity accelerated the surface precipitation of casting solution and a much more viscous layer was formed on top. Slow de-mixing rate caused by this viscous layer resulted with more "sponge-like" membrane morphology. Regarding lab scale membrane manufacturing where casting and coagulation were conducted in different places, more asymmetric structures are expected at higher coagulation bath temperatures. On the other hand, in pilot scale, casting and coagulation is a continuous process. Casting solution is directly exposed to humidity around the coagulation bath and therefore phase inversion kinetics was affected. Especially M9 and M11 membranes have macro voids as seen in their cross-section SEM images. Macro voids are generally formed under instantaneous de-mixing conditions, if the polymer additive concentration and the non-solvent concentration in the polymer solution do not exceed a particular value [38,43–45]. In case of low coagulation bath temperature, M9 and M11 membranes were less affected from humidity and instantaneous de-mixing was took place. This is why more macro voids are formed.

3.2. Pore size distribution of membranes

Pore size distributions of the casted membranes are given in Fig. 5. Calculated mean pore sizes are given in Table 3. Since no pores were observed from M1 and M2, these membranes are not included in Fig. 5. As stated before, pore sizes and pore size distribution are affected from solvent to non-solvent de-mixing rate. When de-mixing rate increased, small pores and narrower pore size distribution is expected.

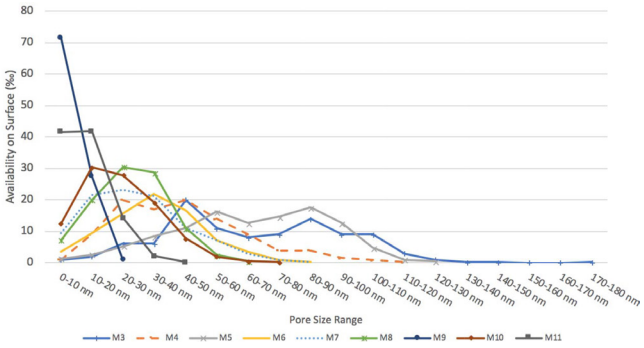

Fig. 5. Pore size distribution of membranes.

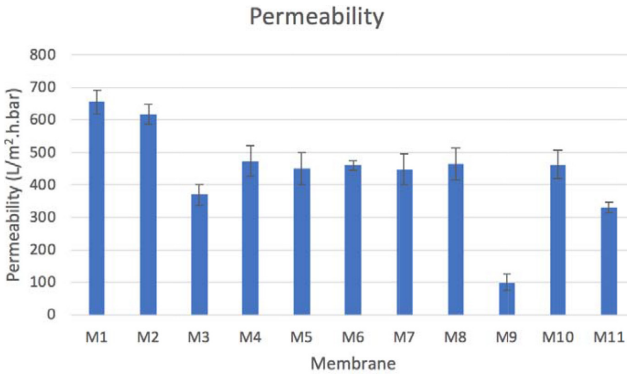

Fig. 6. Permeability of membranes.

Table 3
Mean pore sizes and standart deviations

Membrane	Mean pore size (nm)	+/– (nm)	Classification
M3	63	28	Microfiltration
M4	42	21	Ultrafiltration
M5	60	25	Microfiltration
M6	40	17	Ultrafiltration
M7	29	15	Ultrafiltration
M8	27	11	Ultrafiltration
M9	8	4	Ultrafiltration
M10	24	12	Ultrafiltration
M11	13	7	Ultrafiltration

This phenomenon can be observed in membranes that casted with increasing casting speed rates and decreasing coagulation bath temperatures. In lab scale, decreasing the coagulation bath temperature should lead to bigger pore sizes and sponge-like structures whereas in pilot scale, coagulation bath temperature and humidity around coagulation bath affected phase inversion as explained in detailed before.

Addition of PVP into casting solutions led to different membrane morphologies and pore structure as well [46]. It was found that the addition of PVP led to increase in viscosity. Solution viscosity affects solvent-non-solvent exchange rate. Jung et al. summarized that, when PVP amount was increased, top layer of membranes became thicker and the number of finger-like macro voids gradually disappeared in the membrane [47]. In the direction of green arrow, from M5 to M7, PVP concentration in solution decrease and membrane pore sizes were decreased and narrower pore size distribution was obtained supported by SEM images as well. One possible explanation for this is the decreased solution viscosity caused enhanced phase inversion resulted in an increase in polymer-rich phase on the membrane surface having tighter pores. Another possible explanation was the leaching of PVP from membrane matrix brought about pore formation. M5 membrane had PVP having 40 kDa molecular weight in the membrane matrix, whereas M6 did not have. PVP40 can help to form much more bigger pores.

Chakrabarty et. al. [19] have found that membrane skin layers are thicker and voids in membrane structure are less when PVP concentration increased. PVP can be washed out successfully from membrane matrix using hypochlorite [47]. However in this study due to low concentration and molecular weight of PVP, no hypochlorite treatment was done.

3.3. Permeability of membranes

Permeabilities of membranes are given in Fig. 6. Membrane permeabilities were decreased from M1 to M4 where casting speed was increased and evaporation time was decreased,. Permeability is mainly affected by membrane resistance to passage of water. If membrane pore size decreases and sponge-like structure increases, resistance of membrane to water pass increases as well. Membrane permeabilities are generally decreased by decreasing coagulation bath temperatures as can be seen in M10 to M11, M4 to M5 and M8 to M9. It can be concluded that, increased casting speed led to decrease in pure water permeability of support membranes.

4. Conclusions

This study provides a detailed insight into the fabrication of asymmetric membranes which can be used as support membranes in thin film composite membranes. Main finding of this study is that, optimization of membrane fabrication for lab scale and pilot scale can be quite different from each other since one is batch system and the other is continuous system. Lab scale conditions given in literature cannot be always applied for pilot or industrial scale. Each parameter affects membrane structures in a combined way in pilot scale. It has been found that, coagulation bath temperature affects humidity around pilot scale membrane manufacturing line. Consequently temperature around the bath affects membrane structure. Several type support membranes with different pore size and morphologies have been successfully fabricated in this study.

Acknowledgments

This work was supported by the Scientific and Technological Research Council of Turkey (TUBITAK) [grant number 113Y356].

References

[1] J.E. Cadotte, R.J. Petersen, Synthetic membranes, ACS publications; 1981. Chapter 21, Thin-film composite reverse-osmosis membranes: Origin, development, and recent advances, pp. 305–326.

[2] J. Lee, R. Wang, T.-H. Bae, High-performance reverse osmosis membranes fabricated on highly porous micro structured supports, Desalination, 436 (2018) 48–55.

[3] J. Xu, H. Yan, Y. Zhang, G. Pan, Y. Liu, The morphology of fully-aromatic polyamide separation layer and its relationship with separation performance of TFC membranes, J. Membr. Sci., 541 (2017) 174–188.

[4] Q. Zhang, Z. Zhang, L. Dai, H. Wang, S. Li, S. Zhang, Novel insights into the interplay between support and active layer in the thin film composite polyamide membranes, J. Membr. Sci., 537 (2017) 372–383.

[5] J. Ren, M.R. Chowdhury, J. Qi, L. Xia, B.D. Huey, J.R. McCutcheon, Relating osmotic performance of thin film composite hollow fiber membranes to support layer surface pore size, J. Membr. Sci., 540 (2017) 344–353.

[6] J.E. Cadotte, Inter facially synthesized reverse osmosis membrane, US Patent 4,277,344, (1981).

[7] M. Mulder, Basic principles of membrane technology; Kluwer Academic Publishers: Dordrecht, The Netherlands, 2003.

[8] N. Koutahzadeh, M.R. Esfahani, H.A. Stretz, P.E. Arce, Investigation of UV/H_2O_2 pretreatment effects on humic acid fouling on polysulfone/titanium dioxid and polysulfone/multi wall carbon nano tube Nano composite Ultrafiltration membranes, Environ. Progr. Sustain. Energy, 36–1 (2017) 27–37.

[9] N. Koutahzadeh, M.R. Esfahani, P.E. Arce, Sequential use of UV/H_2O_2-(PSF/TiO_2/MWCNT) mixed matrix membranes for dye removal in water purification: Membrane permeation, fouling, rejection, and decolorization, Environ. Eng. Sci., 33–6 (2016) 430–440.

[10] M. Sile-Yuksel, B. Tas, D.Y. Koseoglu-Imer, I. Koyuncu, Effect of silver nanoparticle (AgNP) location in nanocomposite membrane matrix fabricated with different polymer type on antibacterial mechanism, Desalination, 347 (2016) 120–130.

[11] G.R. Guillen, Y. Pan, M. Li, E.M.V. Hoek, Preparation and characterization of membranes formed by nonsolvent ınduced phase separation: a review, Ind. Eng. Chem. Res., 50(7) (2011) 3798–3817.

[12] N.-N. Bui, M.L. Lind, E.M.V. Hoek, J.R. McCutcheon, Electrospun nanofiber supported thin film composite membranes for engineered osmosis, J. Membr. Sci., 385–386 (2011) 10–19.

[13] H.A. Tsai, R.C. Ruaan, D.M. Wang, J.Y. Lai, Effect of temperature and span series surfactant on the structure of polysulfone membranes, J. Appl. Polym. Sci., 86 (2002) 166–173.

[14] M.J. Han, S.T. Nam, Thermodynamic and rheological variation in polysulfone solution by PVP and its effect in the preparation of phase inversion membrane, J. Membr. Sci., 202 (2002) 55–61.

[15] B. Chakrabarty, A.K. Ghoshal, M.K. Purkait, Effect of molecular weight of PEG on membrane morphology and transport properties, J. Membr. Sci., 309 (2008) 209–221.

[16] Q.Z. Zheng, P. Wang, Y.N. Yang, Rheological and thermodynamic variation in polysulfone solution by PEG introduction and its effect on kinetics of membrane formation via phase-inversion process, J. Membr. Sci., 279 (2006) 230–237.

[17] A.L. Ahmad, M. Sarif, S. Ismail, Development of an integrally skinned ultrafiltration membrane for wastewater treatment: Effect of different formulations of PSf/NMP/PVP on flux and rejection, Desalination, 179 (2005) 257–263.

[18] M.J. Han, Effect of propionic acid in the casting solution on the characteristics of phase inversion polysulfone membranes, Desalination, 121 (1999) 31–39.

[19] B. Chakrabarty, A.K. Ghoshal, A.K. Purkait, Preparation, characterization and performance studies of polysulfone membranes using PVP as an additive, J. Membr. Sci., 315 (2008) 36–47.

[20] Q.Z. Zheng, P. Wang, Y.N. Yang, D.J. Cui, The relationship between porosity and kinetics parameter of membrane formation in PSF ultrafiltration membrane, J. Membr. Sci., 286 (2006) 7–11.

[21] T.P. Hou, S.H. Dong, L.Y. Zheng, The study of mechanism of organic additives action in the polysulfone membrane casting solution, Desalination, 83 (1991) 343–360.

[22] M. Fontyn, K. Vantriet, B.H. Bijsterbosch, Surface spectroscopic studies of pristine and fouled membranes. 1. Method development and pristine membrane characterization, Colloids Surf., 54 (1991) 331–347.

[23] C. Barth, M.C. Goncalves, A.T.N. Pires, J. Roeder, B.A. Wolf, Asymmetric polysulfone and polyether sulfone membranes: Effects of thermodynamic conditions during formation on their performance, J. Membr. Sci., 169 (2000) 287–299.

[24] L. Xue, Z. Sui, F. Fengjiang, T.-S. Chung, Deformation and reinforcement of thin-film composite (TFC) polyamide-imide (PAI) membranes for osmotic power generation, J. Membr. Sci., 434 (2013) 204–217.

[25] F.G. Paulsen, S.S. Shojaie, W.B. Krantz, Effect of evaporation step on macro void formation in wet-cast polymeric membranes, J. Membr. Sci., 91 (1994) 265–282.

[26] L. Zeman, T. Fraser, Formation of air-cast cellulose-acetate membranes 1. Study of macro void formation, J. Membr. Sci., 84 (1993) 93–106.

[27] H. Strathmann, K. Kock, P. Amar, R.W. Baker, The formation mechanism of asymmetric membranes, Desalination, 16 (1975) 179–203.

[28] H. Strathmann, K. Kock, Formation mechanism of phase inversion membranes, Desalination, 21 (1977) 241–255.

[29] R.E. Kesting, A.K. Fritzsche, Polymeric gas separation membranes, Wiley, New York, 1993.

[30] S.S. Madaeni, A. Rahimpour, M. Barzin, Preparation of polysulphone Ultrafiltration membranes for milk concentration: effect of additives on morphology and performance, Iran. Polym. J., 14 (2005) 421–428.

[31] J. Barzin, S.S. Madaeni, H. Mirzadeh, M. Mehrabzadeh, Effect of polyvinylpyrolidone on morphology and performance of hemodialysis membranes prepared from polyether sulfone, J. Appl. Polym. Sci., 92 (2004) 3804–3813.

[32] A. Bottino, G. Camera-Roda, G. Capannelli, S. Munari, The formation of micro porous polyvinylidene difluoride membranes by phase-separation, J. Membr. Sci., 57 (1991) 1–20.

[33] C. Friedrich, A. Driancourt, C. Noel, L. Monnerie, Asymmetric reverse-osmosis and ultrafiltration membranes prepared from sulfonated polysulfone, Desalination, 36 (1981) 39–62.

[34] P. Neogi, Mechanism of pore formation in reverse-osmosis membranes during the casting process, AIChE J., 29 (1983) 402–410.

[35] D.M. Wang, F.C. Lin, T.T. Wu, J.Y. Lai, Formation mechanism of the macro voids induced by surfactant additives, J. Membr. Sci., 142 (1998) 191–204.

[36] F.C. Lin, D.M. Wang, C.L. Lai, J.Y. Lai, Effect of surfactants on the structure of PMMA membranes, J. Membr. Sci., 123 (1997) 281–291.

[37] Y.S. Kang, H.J. Kim, U.Y. Kim, Asymmetric membrane formation via immersion precipitation method 1. Kinetic effect, J. Membr. Sci., 60 (1991) 219–232.

[38] R.M. Boom, I.M. Wienk, T. Vandenboomgaard, C.A. Smolders, Micro structures in phase inversion membranes 2. The role of a polymeric additive, J. Membr. Sci., 73 (1992) 277–292.

[39] R.M. Boom, T. Vandenboomgaard, C.A. Smolders, Mass-transfer and thermo-dynamics during immersion precipitation for a 2-polymer system—evaluation with the system PES–PVP–NMP–water, J. Membr. Sci., 90 (1994) 231–249.

[40] R. Sengur, C.-F. de Lannoy, T. Turken, M. Wiesner, I. Koyuncu, Fabrication and characterization of hydroxylated and carboxylated multi walled carbon nano tube/polyether sulfone (PES) nano composite hollow fiber membranes, Desalination, 359 (2015) 123–140

[41] M.J. Han, P.M. Bummer, M. Jay, D. Bhattacharyya, Phase-transitions of polysulfone solution during coagulation, Polymer., 36 (1995) 4711–4714.

[42] Q.Z. Zheng, P. Wang, Y.N. Yang, D.J. Cui, The relationship between porosity and kinetics parameter of membrane formation in PSF Ultrafiltration membrane, J. Membr. Sci., 286 (2006) 7–11.

[43] C.A. Smolders, A.J. Reuvers, R.M. Boom, I.M. Wienk, Micro structures in phase-inversion membranes. 1. Formation of macro voids, J. Membr. Sci., 73 (1992) 259–275.
[44] K. Kimmerle, H. Strathmann, Analysis of the structure-determining process of phase inversion membranes, Desalination, 79 (1990) 283–302.
[45] J.Y. Lai, C.F. Lin, C.C. Wang, D.M. Wang, Effect of non solvent additives on the porosity and morphology of asymmetric TPX membranes, J. Membr. Sci., 118 (1996) 49–61.
[46] S.H. Yoo, J.H. Kim, J.Y. Jho, J. Won, Y.S. Kang, Influence of the addition of PVP on the morphology of asymmetric polyimide phase inversion membranes: Effect of PVP molecular weight, J. Membr. Sci., 236 (2004) 203–207.
[47] B. Jung, J.K. Yoon, B. Kim, H.W. Rhee, Effect of molecular weight of polymeric additives on formation, permeation properties and hypochlorite treatment of asymmetric polyacrylonitrile membranes, J. Membr. Sci., 243 (2004) 45–57.